Synthesis, X-ray Structure, Single-Crystal EPR and ^{1}H NMR Studies of a Distorted Square Planar Cu(salEen)$_2$(ClO$_4$)$_2$ Complex in a Novel Bilayered Architecture: salEen = *N*,*N*-Diethylethylenesalicylidenamine

P. S. Subramanian, E. Suresh, and D. Srinivas*

Sophisticated Analytical Instruments Laboratory, Central Salt and Marine Chemicals Research Institute, Gijubhai Badheka Marg, Bhavnagar-364 002, India, and Catalysis Division, National Chemical Laboratory, Pune-411 008, India

Received July 23, 1999

Single-crystal X-ray structure and spectroscopic characterizations of Cu(salEen)$_2$(ClO$_4$)$_2$, are reported; salEen is a Schiff base condensation product of equimolar amounts of salicylaldehyde and *N*,*N*-diethylethylenediamine. The complex crystallizes in a triclinic space group $P\bar{1}$ with $a = 12.055(4)$ Å, $b = 10.652(3)$ Å, $c = 12.701(3)$ Å, $\alpha = 90.54(2)°$, $\beta = 94.39(2)°$, $\gamma = 91.35(3)°$, and $Z = 2$. The coordination geometry around Cu(II) ion is tetrahedrally distorted square planar with salEen coordinating as a neutral bidentate ligand through N and O donor atoms (average Cu−N and Cu−O distances are 2.004 and 1.880 Å, respectively). The counterion ClO_4^- makes H-bonding contacts with the neighboring cation moieties and forms a one-dimensional layered arrangement of the molecules. The pendent, *N*,*N*-diethylethylenediamine groups of salEen (from the centrosymmetrically related molecules) in adjacent layers interpenetrate, forming novel bilayered architectures, which are further held together by $\pi-\pi$ stacking interactions. EPR studies on single crystals, in three mutually orthogonal planes, yield a rhombic **g** tensor ($g_x = 2.041(1)$, $g_y = 2.073(1)$, and $g_z = 2.220(1)$) consistent with the distorted square planar geometry of the CuN_2O_2 moiety. The peak-to-peak line width of the EPR signal exhibits a $|3\cos^2\theta - 1|^{4/3}$ variation, attributable to one-dimensional magnetic exchange behavior of the complex. The analysis suggests that both the dipole−dipole and exchange interactions contribute to the line width. Interestingly, the complex is amenable for both EPR and NMR studies at ambient temperatures. The proton NMR signals are narrow in CD_3CN solutions and the HOMO correlation spectroscopy (COSY) studies reveal the ^{1}H connectivities. Nuclear spin lattice relaxation time (T_1) measurements, using inversion recovery method, indicate that T_1 values for all the protons are remarkably long compared to those of other mononuclear Cu(II) complexes.

Introduction

Copper(II) is known to form complexes with a variety of molecular geometries (e.g., tetrahedral, square planar, square pyramidal, and octahedral).[1] Further, copper is a bioelement and an active site in several metalloenzymes and proteins.[2−4] Among these, the blue copper proteins have received considerable interest because of their unusual spectral and structural properties.[2,4] The geometry around copper in blue copper proteins is intermediate between tetrahedral and square planar. Several model systems, including those with bidentate Schiff base ligands, have been reported correlating the molecular structure with the electronic ground state of those complexes.[5,6] Our earlier reports on tetradentate salen complexes of Cu(II)[7] and those by Ratnasamy et al.[8] on the zeolite-encapsulated complexes revealed higher activity for the chloro-substituted complex, which has a tetrahedrally distorted square planar geometry. In the course of understanding the structure−function relationships, we report here the synthesis, crystal and molecular structure, and single-crystal EPR studies of Cu(salEen)$_2$(ClO$_4$)$_2$, where salEen = *N*,*N*-diethylethylenesalicylidenamine. The salEen ligand coordinates in a bidentate fashion through N and O donor atoms. The diethyl-substituted end of the amine group is left free and participates in intermolecular interactions, forming large porous cavity structures. The novelty of this molecule is the distorted square planar geometry and bilayered architecture. Interestingly, this bimolecular association is stable even in solutions. Single-crystal EPR studies reveal one-dimensional magnetic behavior. The counterion, perchlorate, mediates the intermolecular exchange interactions. It is pertinent to note that one-dimensional materials are receiving continuing interest because of their potential as molecular-based ferromagnets, synthetic metal conductors, nonlinear optical (NLO) materials,

* To whom correspondence should be addressed. Address: Catalysis Division, National Chemical Laboratory, Pune-411 008, India. E mail: srinivas@cata.ncl.res.in. Fax: (91)-20-5893761.

(1) Hathaway, B. J. In *Comprehensive Coordination Chemistry*; Wilkinson, G., Gillard, R. D., McCleverty, J. A., Eds.; Pergamon Press: Oxford, 1987; Vol. 5, Chapter 53, p 558.
(2) Solomon, E. I.; Penfield, K. W.; Wilcox, D. E. *Struct. Bonding* **1983**, *53*, 1−57. Penfield, K. W.; Gay, R. R.; Himmelwright, R. S.; Eickman, N. C.; Norris, V. A.; Freeman, H. C.; Solomon, E. I. *J. Am. Chem. Soc.* **1981**, *103*, 4382.
(3) Abolmaali, B.; Taylor, H. V.; Weser, U. *Struct. Bonding* **1998**, *91*, 91−190.
(4) Messerschmidt, A. *Struct. Bonding* **1998**, *90*, 37−68. Messerschmidt, A. Blue Copper Oxidases. *Adv. Inorg. Chem.* **1994**, *40*, 121−185. Sykes, A. G. Active-site properties of the Blue copper proteins. *Adv. Inorg. Chem.* **1991**, *36*, 377−408.
(5) Bertini, I.; Canti, G.; Grassi, R. *Inorg. Chem.* **1980**, *19*, 2198.
(6) Yokoi, H.; Addison, A. W. *Inorg. Chem.* **1977**, *16*, 1341. Yokoi, H. *Bull. Chem. Soc. Jpn.* **1974**, *47*, 3037.
(7) Bhadbhade, M. M.; Srinivas, D. *Inorg. Chem.* **1993**, *32*, 5458.
(8) Jacob, C. R.; Varkey, S. P.; Ratnasamy, P. *Microporous Mesoporous Mater*. **1998**, *22*, 465. Jacob, C. R.; Varkey, S. P.; Ratnasamy, P. *Appl. Catal. A* **1998**, *168*, 353.

10.1021/ic990874q CCC: $19.00
Published on Web 04/15/2000

and ferroelectric materials.[9] Copper complexes are generally not amenable for NMR studies because of paramagnetism and unfavorable relaxation times.[10,11] However, the present complex exhibits sharp NMR signals at ambient temperatures. An analogous Cu(II) complex with *N*,*N*-dimethyl substitution was reported by Das et al.[12] in which the Schiff base coordinates as a tridentate ligand. The Cu(II) complex exhibits catalytic activity for the epoxidation of alkenes using molecular oxygen.[12,13] The details of the crystal structure, molecular association, EPR line width, and line shape anisotropies and proton relaxation times of the title complex are discussed.

Experimental Section

Materials. $CuSO_4 \cdot 5H_2O$, *N*,*N*-diethylethylenediamine, and $NaClO_4$ obtained from Aldrich Co. were used as received. The solvents employed were of A.R. grade and purified further by standard procedures.[14]

Synthesis. To an ethanolic solution of *N*,*N*-diethylethylenediamine (1 mmol, 25 mL) was added an equimolar amount of salicylaldehyde (1 mmol) in small fractions, and the mixture was stirred overnight at 323 K. The orange, oily condensation product thus formed was characterized by ^{1}H NMR. ^{1}H chemical shifts (ppm): 13.07 (s, OH), 8.36 (s, CH), 7.37, 7.29, 7.22 (t, phenyl), 6.98, 6.93, 6.90, 6.78 (m, phenyl), 3.81, 3.74, 3.67 (t, ethylenic CH_2), 2.89, 2.83, 2.76, 2.69, 2.62, 2.54 (m, ethylenic and ethyl CH_2) and 1.15, 1.07, 1.00 (t, CH_3).

$Cu(salEen)_2(ClO_4)_2$ was synthesized by adding dropwise an aqueous solution of $CuSO_4 \cdot 5H_2O$ (0.5 mmol, 10 mL) to the above condensation product while stirring at 323 K. To this was added $NaClO_4$ (1 mmol) in 10 mL of ethanol, and the resultant dark-green solution of the complex was kept for slow evaporation. Good quality single crystals were obtained in 10 days. Anal. Calcd for $CuC_{26}N_4H_{40}Cl_2O_{10}$: C, 44.41; H, 5.69; N, 7.97. Found: C, 44.29; H, 5.81; N, 7.76.

Caution! Perchlorate salts of metal complexes are potentially explosive and should be handled with great care.

Physical Measurements. Microanalysis of the complex was done using a Perkin-Elmer PE 2400 series II CHNS/O elemental analyzer. Electronic spectra were recorded in various solvents by using a Shimadzu UV−visible spectrophotometer (UV-160 A).

EPR investigations were performed on a Bruker EMX X-band spectrometer with a field modulation of 100 kHz, modulation amplitude of 2 G, and microwave radiation power of 2 mW. Spectra for solutions, at 298 K, were recorded using a quartz aqueous cell, and the measurements at 77 K were done using a quartz finger Dewar. DPPH was used as a field marker ($g_{iso} = 2.0036$). The spectra for single crystals were recorded in three mutually perpendicular planes at 10° intervals. Spectral simulations were carried out using a Bruker Simfonia software package.

FT-NMR spectra were recorded on a Bruker 200 MHz DPX Avance spectrometer. TMS was used as an internal reference. Dissolved oxygen was prevented by purging the solvents with zero-grade nitrogen gas before proceeding with NMR experiments. Spin−lattice relaxation time (T_1) measurements were carried out using a Bruker XWIN NMR software package, which is based on the inversion recovery technique consisting of the following train of pulse sequences[15]

$$(180°-\tau-90°-\mathrm{Aq}-\mathrm{D})_n$$

where Aq is the acquisition time, *D* is the delay to allow equilibrium to be reached, and 8.9 μs is the calibrated 90° pulse. The values of magnetization, which are directly related to NMR signal intensity, vary from $-M_z(0)$ when $\tau = 0$ to $M_z(\infty)$ when $\tau = 5T_1$, and τ is the variable time delay between the two pulses. It is possible to relate the magnetization to the T_1 values by the following equation:

$$M_z(\tau) = M_z(\infty)[1 - 2\exp(-\tau/T_1)] \quad (1)$$

T_1, therefore, can be calculated by a least-squares fit analysis of the experimental magnetization data as a function of τ.

Table 1. Crystallographic Data for $Cu(salEen)_2(ClO_4)_2$

chemical formula	$C_{26}H_{40}Cl_2N_4O_{10}Cu$	fw	721.26
a	12.055(4) Å	cryst syst	triclinic
b	10.652(3) Å	space group	*P*1 (No. 2)
c	12.701(3) Å	*T*	25 °C
α	90.54(2)°	λ	0.7107 Å
β	94.39(2)°	ρ_{calcd}	1.473 g cm^{-3}
γ	91.35(3)°	μ	8.98 cm^{-1}
V	1625.6(8) Å^3	$R(F_0^2)^a$	0.089
Z	2	$R_w(F_0^2)^a$	0.220

^{a} $R = \sum||F_o| - |F_c||/\sum|F_o|$; $R_w = [\sum w(F_o^2 - F_c^2)^2]/\sum[w(F_o^2)^2]^{1/2}$; $w = 1/\sigma(F_0)^2$.

X-ray Crystallography. X-ray diffraction data for the complex were collected at 298 K, with an Enraf-Nonius CAD-4 diffractometer, using monochromatic Mo Kα radiations (0.7107 Å), in the θ range 2−25°. Unit cell parameters were determined from a least-squares refinement of the setting angles of 25 reflections with 2θ in the range 24−28°. A summary of crystallographic data is given in the Table 1. Three reference reflections monitored throughout the data collection showed no intensity loss for the complex. The structure was solved by the heavy-atom method using the program SHELX-97[16] and refined by the full matrix least-squares procedures. The crystal orientation, refinement of cell parameters, and intensity measurements were carried out using the program CAD-4 PC.[17] Intensities were corrected for Lorentz polarization effects but not for absorption. The Lorentz polarization correction and data reduction were carried out using the NRCVAX program.[18]

Extensive disorder of one of the ClO_4^- anions was observed at the structure solution stage itself. After all the non-H atoms of the cation and one of the perchlorate anions were located in the Fourier difference map, the peak for the other perchlorate chlorine appeared with a height of ∼16 e Å^{-3}, while large number of peaks appeared with heights ranging from 2.0 to 1.2 e Å^{-3} joining the chlorine atom, which correspond to the disordered oxygen atoms. Anisotropic full-matrix refinement of all atoms, except the disordered oxygen atoms attached to Cl2, was carried out using SHELX-97[16] until convergence was reached. Attempts to resolve the orientational disorder of ClO_4^- was not possible because a large number of peaks with heights ∼1.8 e Å^{-3} appeared in the difference Fourier map. Therefore, all the peaks with heights greater than 1.3 e Å^{-3} were included at every stage, only for the structural factor contribution in the least-squares refinement, until the difference Fourier map contained no significant peaks corresponding to oxygen atoms. Hydrogen atoms were either obtained from the difference Fourier map or included in fixed, idealized positions by a

(9) Chen, C.-I. Suslick, K. S. *Coord. Chem. Rev*. **1993**, *128*, 293 and references therein.
(10) *NMR of Paramagnetic Molecules: Principles and Applications*; La Mar, G. N., Horrocks, W. DeW., Jr., Holm, R. H., Eds.; Academic Press: New York, 1973. Bertini, I.; Luchinat, C. *NMR of Paramagnetic Molecules in Biological Systems*; Benjamin & Cummings: Menlo Park, CA 1986.
(11) Brink, J. M.; Rose, R. A.; Holz, R. C. *Inorg. Chem.* **1996**, *35*, 2878. Satcher, J. H., Jr.; Balch, A. L. *Inorg. Chem.* **1995**, *34*, 3371. Lubben, M.; Hage, R.; Meetsma, A.; Byma, K.; Feringa, B. L. *Inorg. Chem.* **1995**, *34*, 2217. Mandal, P. K.; Manoharan, P. T. *Inorg. Chem.* **1995**, *34*, 270. Holz, R. C.; Brink, J. M. *Inorg. Chem.* **1994**, *33*, 4609. Maekawa, M.; Kitagawa, S.; Munakata, M.; Masuda, H. *Inorg. Chem.* **1989**, *28*, 1904. Holz, R. C.; Bennett, B.; Chen, G.; Ming, L.-J. *J. Am. Chem. Soc.* **1998**, *120*, 6329.
(12) Das, G.; Shukla, R.; Mandal, S.; Singh, R.; Bharadwaj, P. K.; van Hall, J.; Whitmira, L. H. *Inorg. Chem.* **1992**, *36*, 323.
(13) Yamada, T.; Takai, T.; Rhode, O.; Mukaiyama, T. *Chem. Lett.* **1991**, 1.
(14) Perrin, D. D.; Armarego, W. L. F.; Perrin, D. R. *Purification of Laboratory Chemicals*; Pergamon Press: Oxford, 1980.
(15) Becker, E. D. *High Resolution NMR*; Academic Press: New York, 1969.
(16) Sheldrick, G. M. *SHELX-97, Program For The Solution Of Crystal Structures*; University of Göttigen: Göttingen, Germany, 1997.
(17) *CAD-4 PC Software*, version 5; Enraf-Nonius: Delft, The Netherlands, 1989.
(18) Gabe, E. I.; Le Page, Y.; Charland, I. P.; Lee, F. L.; White, P. S. *J. Appl. Crystallogr*. **1989**, *22*, 384.

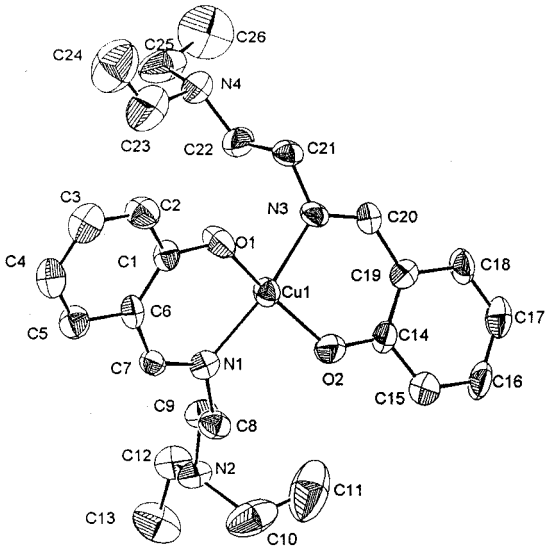

Figure 1. ORTEP view of $Cu(salEen)_2(ClO_4)_2$. Vibrational ellipsoids are drawn at the 40% probability level.

Table 2. Selected Bond Lengths [Å] and Angles [deg] for $Cu(salEen)_2(ClO_4)_2$

Cu(1)−O(2)	1.879(6)	Cu(1)−O(1)	1.887(5)
Cu(1)−N(1)	1.998(6)	Cu(1)−N(3)	2.011(6)
O(1)−C(1)	1.310(8)	O(2)−C(14)	1.311(9)
N(1)−C(7)	1.301(9)	N(1)−C(8)	1.444(10)
N(3)−C(20)	1.316(9)	N(3)−C(21)	1.438(10)
C(19)−C(20)	1.418(10)	C(19)−C(14)	1.424(11)
C(6)−C(1)	1.378(10)	C(6)−C(7)	1.440(10)

O(2)−Cu(1)−O(1)	157.2(3)	O(2)−Cu(1)−N(3)	92.9(3)
O(2)−Cu(1)−N(1)	90.6(2)	O(1)−Cu(1)−N(1)	92.8(2)
O(1)−Cu(1)−N(3)	91.5(3)	N(1)−Cu(1)−N(3)	160.2(2)
C(1)−O(1)−Cu(1)	129.8(5)	C(14)−O(2)−Cu(1)	130.6(5)
C(7)−N(1)−C(8)	115.0(7)	C(8)−N(1)−Cu(1)	121.9(6)
C(7)−N(1)−Cu(1)	123.1(5)	C(20)−N(3)−C(21)	116.7(7)
C(20)−N(3)−Cu(1)	122.5(6)	C(21)−N(3)−Cu(1)	120.8(6)
C(20)−C(19)−C(14)	123.4(7)	C(1)−C(6)−C(7)	124.3(7)
N(1)−C(7)−C(6)	126.5(7)	O(1)−C(1)−C(6)	123.2(7)
N(3)−C(20)−C(19)	127.7(8)	O(2)−C(14)−C(19)	122.8(7)

riding model using the program SHELX-97.[16] At this stage 16 peaks corresponding roughly to four major orientations of ClO_4^- with occupancy 0.25 were allowed to refine isotropically, while the rest of the non-H atoms were refined using the weighting scheme $w = 1/\sigma(F_0^2)^2$. The inclusion of all the 16 disordered O atoms significantly reduced the refinement parameters such as R, R_w, and goodness of fit, implying the correct treatment of the anion disorder, although a constrained or rigid model refinement was not possible in this case.

Results

X-ray Structure and Molecular Association of $Cu(salEen)_2(ClO_4)_2$. An ORTEP[19] view of the complex cation is shown in Figure 1 along with the atom numbering. Selected bond lengths and angles are listed in Table 2. The metal center possesses a tetrahedrally distorted square planar geometry with N_2O_2 donor atoms coordination from two different salEen ligand moieties. The Schiff base ligand is present as a neutral species with the charge on the metal ion balanced by two perchlorate ions outside the coordination sphere. Even though the ligand is tridentate in nature, it binds to the Cu(II) ion in a bidentate fashion through the OH of the phenyl ring and nitrogen of the azomethine group, leaving the diethyl-substituted terminal nitrogen free. The bidentate coordination of the ligand can be attributed to the steric strain imparted by the diethyl substitution at the terminal nitrogens N2 and N4. The Cu−N distances (Cu1−N1 = 1.996(6) Å; Cu1−N3 = 2.011(6) Å) are well within the range reported for the related Schiff base complexes of Cu(II) salen.[7] The Cu−O distances (Cu1−O1 = 1.884(5) Å; Cu1−O2 = 1.876(5) Å) are shorter compared to those of Cu(salen) complexes,[7] even though in the present case the protonated OH group is coordinated to the metal center. This may be due to the closer approach of the ligand moiety to form much stronger six membered (O2−C14−C19−C20−N3 and O1−C1−C6−C7−N1) chelate rings with the Cu(II), while the *N*,*N*-diethylethylenediamino substitutent is left free. The cis angles subtended by the six-membered chelate ring with Cu(II) from each ligand (O1−Cu1−N1 = 92.8(2)°, O2−Cu1−N3 = 92.9(2)°, O2−Cu1−N1 = 90.4(2)°, O1−Cu1−N3 = 91.7(2)°) deviate only marginally from the ideal square planar value. However, the trans angles (N1−Cu1−N3 = 160.2(2)° and O2−Cu1−O1 = 157.2(2)°) at the Cu(II) center deviate considerably from an ideal square planar geometry, indicating a tetrahedral bias to the Cu(II) coordination. This may be due to the steric constraints imposed by the long flexible side chain for the right approach toward the metal for coordination. This is further strengthened by the mean plane involving the "sal" units from different ligands, which are twisted relative to each other by approximately 146.3° and make angles of 167.5° (C1 to C7 and O1) and 36.2° (C14 to C20 and O2) with respect to the N_2O_2 mean plane. The N and O atoms show considerable deviation from the mean plane involving N_2O_2; both the trans oxygens from two different salEen moieties (O1 = −0.356 Å and O2 = −0.361 Å) and the trans nitrogens (N1 = 0.362 and N3 = 0.355) are displaced in the same direction; the metal center is contained well within the plane (Cu1 = 0.011 Å). It is pertinent to note such a distortion in the Cu(II) geometry in blue copper proteins. The catalytic activity of alkylsalicylidenaminatoCu(II) complexes could be attributed to the distortion from the square planar geometry, which results in an admixed electronic ground state.[17,18]

Both bidendate salEen ligands are coordinated in the same fashion with the Cu(II), but the conformations of the aliphatic chains attached to the azomethine nitrogens N1 and N3 are quite different. The ethylenediamine collar is almost in an extended conformation for both the ligand moieties (torsion angles N1−C8−C9−N2 = −165.3(1)°, N3−C21−C22−N4 = 164.9(2)°). For the former ligand moiety the torsion angles involving the carbon atoms attached to azomethine nitrogen N1 (C8, C9), the terminal nitrogen N2, and the ethyl carbons (C12 and C13) are almost in an extended conformation (torsion angles C8−C9−N2−C12 = 172.6(5)°, C9−N2−C12−C13 = −171.1(3)°), whereas the other ethyl carbons (C10 and C11) connected to N2 are in a folded form (torsion angles C8−C9−N2−C10 = −57.2(4)°, C9−N2−C10−C11 = −63.9(5)°). In the case of the second salEen ligand similar comparison of the torsion angles shows marked differences. The torsion angles (C21−C22−N4−C23 = −77.59(5)°, C22−N4−C23−C24 = 162.9(4)°, C21−C22−N4−C25 = 162.6(3)°, C22−N4−C25−C26 = −73.1(8)°) clearly indicate that the ethyl groups attached to N4 are rotated with respect to each other, making a folded chain in which C23 is away from the connecting chain from N4 while C24 makes an approximately good extended steriochemistry with the rest of the three atoms C23, N4, and C22. This trend is just the reverse for the other ethyl group (C25, C26) with N4, C21, and C22.

The packing diagram viewed down the *a* axis is shown in Figure 2. The cationic part of the complex is packed in bilayers

(19) Jhonson, C. K. *ORTEP*; Report ORNL-3794; Oak Ridge National Laboratory: Oak Ridge, TN, 1976.

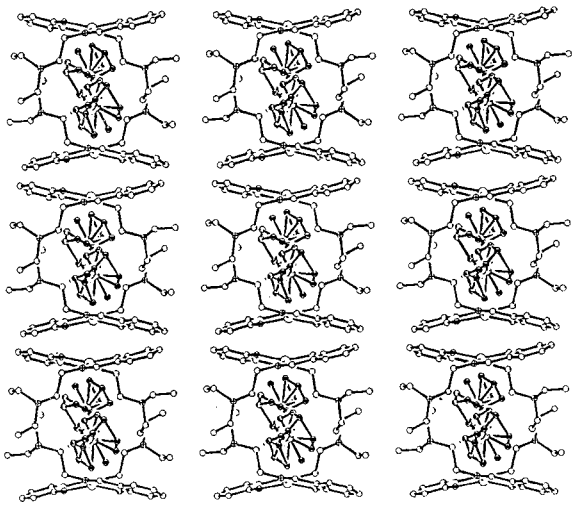

Figure 2. Packing diagram of $Cu(salEen)_2(ClO_4)_2$ viewed down the *a* axis showing the molecular association and the novel bilayered molecular architecture. The pendent *N*,*N*-diethylethylenediamine groups from adjacent layers interpenetrate, creating cavities to accommodate perchlorate anion as a guest molecule.

along the *bc* plane with good stacking interactions of the "sal" moieties. The free N-diethyl groups of the coordinated ligand for the centrosymmetric molecule in the unit cell interpenetrate to form a bilayer with a cavity to encapsulate the disordered perchlorate anion. The disordered perchlorate makes a large number of C−H···O interactions varying from 2.6 to 3.5 Å. The stable perchlorate anion that is at the exterior of the channels interconnects the neighboring molecules to form layered structures via strong C−H···O intermolecular H-bonding with the adjacent diethyl H atoms. This interconnectivity through the perchlorate anion is perhaps responsible for the one-dimensional magnetic behavior observed in single-crystal EPR studies (vide infra). The H-bonding interactions and symmetry code is summarized below. The $\pi\cdots\pi$ stacking of the phenyl group, C−H···O interactions of the stable perchlorate, and C−H···O short contacts by the disordered perchlorate anion play a vital role in the stabilization of the molecule in the crystal lattice and also for the weak exchange interactions.

H-bonding	D−H (Å)	H···O (Å)	D···A (Å)	∠D−H···O (deg)	symmetry code
C24−H243···O5	0.960	2.577	3.516	165.89	$x, y, z+1$
C10−H102···O3	0.969	2.556	3.505	166.01	$-x, 1-y, -z$

Electronic Spectra. The complex is soluble in several solvents and showed two characteristic UV−visible bands, one near 370 nm and the other a relatively weak, broad band with a band maximum in the range 598−642 nm. The former is attributed to $n-\pi^*$ and $\pi-\pi^*$ transitions of ligand origin while the latter to d−d transitions. The solvent has little effect on the ligand-centered band, while the d−d band shifts to the lower energy side in the order CH_3CN < DMF < THF ∼ MeOH ∼ H_2O < DMSO, with increasing σ-donacity of the solvent. The red shift of the d−d transition in DMF, THF, MeOH, H_2O, and DMSO corresponds to solvent coordination and change in copper geometry from distorted square planar to square pyramidal.[1]

EPR Studies. As observed from the single-crystal X-ray structure (vide supra), the molecules of $Cu(salEen)_2(ClO_4)_2$ are self-assembled and form a bilayered one-dimensional architecture through $\pi-\pi$ interactions of "sal" groups and H-bonding interactions via counterion perchlorate and interpenetration of pendent arms forming cavities. The nearest Cu−Cu separations are as follows: intralayer Cu−Cu separation = 6.74 Å, intrabilayer Cu−Cu separation = 9.74 Å, and Cu−Cu separation between adjacent bilayers = 6.49 Å. The exchange interaction is expected to be weak and the intrachain exchange interaction is mediated via counterion perchlorate and H-bonding. EPR spectroscopy has been proved to be a complementary technique to magnetic measurements in such cases.[20−23]

EPR of Polycrystals and Single Crystals. The spectra for the polycrystalline samples of $Cu(salEen)_2(ClO_4)_2$ at 298 and 77 K are similar and correspond to a rhombically distorted **g** tensor. The hyperfine features due to copper could not be resolved because of spin−spin and exchange interactions in the solid state. A typical spectrum at 77 K is shown in Figure 3a.

EPR spectra for single crystals were recorded by rotating the crystal in three mutually orthogonal planes *b***c*, *a***c*, and *a***b**. Although there are two molecules per unit cell, they are magnetically equivalent and thus showed a single line at all the orientations. Representative single-crystal EPR spectra are shown in Figure 4. The angular *g* factor dependence in the *i*th crystal rotation can be described by the general $\mathbf{g}^2$ tensor expression[24, 25]

$$g^2(i) = \alpha_i + \beta_i \cos 2\theta + \gamma_i \sin 2\theta \qquad (2)$$

where θ is the azimuthal angle of the magnetic field. The anisotropy parameters α_i, β_i, and γ_i can be calculated by a least-squares method from the experimental points and from the expressions[26]

$$\alpha_i = n^{-1}\sum_{\theta=0}^{M} g_i^2(\theta)$$

$$\beta_i = 2n^{-1}\sum_{\theta=0}^{M} g_i^2(\theta)\cos 2\theta$$

$$\gamma_i = 2n^{-1}\sum_{\theta=0}^{M} g_i^2(\theta)\sin 2\theta \qquad (3)$$

where $n = 18$ and $M = 170°$ for 10° intervals. The angular variations of *g* values in all the three planes are depicted in Figure 5; the solid line represents the theoretical fit and circles the experimental points. A good fit to the experimental points is seen. The *g* anisotropy is larger in *b***c* and *a***b** planes than in the *a***b* plane. A collection of α_i, β_i, and γ_i parameters for three orthogonal rotations enabled the determination of the $\mathbf{g}^2$ tensor components. The components of the **g** tensor are listed below. The orthorhombicity of the **g** tensor is consistent with the tetrahedrally distorted square planar geometry of the molecule.

$$g_x = 2.041(1), \quad g_y = 2.073(1), \quad g_z = 2.220(1)$$

(20) Bencini, A.; Benelli, C.; Gatteschi, D.; Zanchini, C. *Proc. Indian Acad. Sci., Chem. Sci.* **1987**, *98*, 13.
(21) *Magneto-Structural Correlations in Exchange Coupled Systems*; Gatteschi, D., Khan, O., Willet, R. D., Eds.; NATO Advanced Study Institute Series; Reidel Publishing Co.: Dordrecht, 1985.
(22) Richards, P. M. *Low-Dimensional Cooperative Phenomena*: Keller, H. J., Ed.; Plenum Press: New York, 1975.
(23) Bencini, A.; Gatteschi, D. *EPR of Exchange Coupled Systems*; Springer-Verlag: Berlin, 1990; Chapter 10.
(24) Weil, J. A.; Buch, T.; Clapp, J. E. *Adv. Magn. Reson.* **1973**, *6*, 183.
(25) Waller, W. G.; Rogers, M. T. *J. Magn. Reson.* **1975**, *18*, 39.
(26) Hoffman, S. K.; Corvan, P. J.; Singh, P.; Sethulekshmi, C. N.; Metzger, R. M.; Hatfield, W. E. *J. Am. Chem. Soc.* **1983**, *105*, 4608.

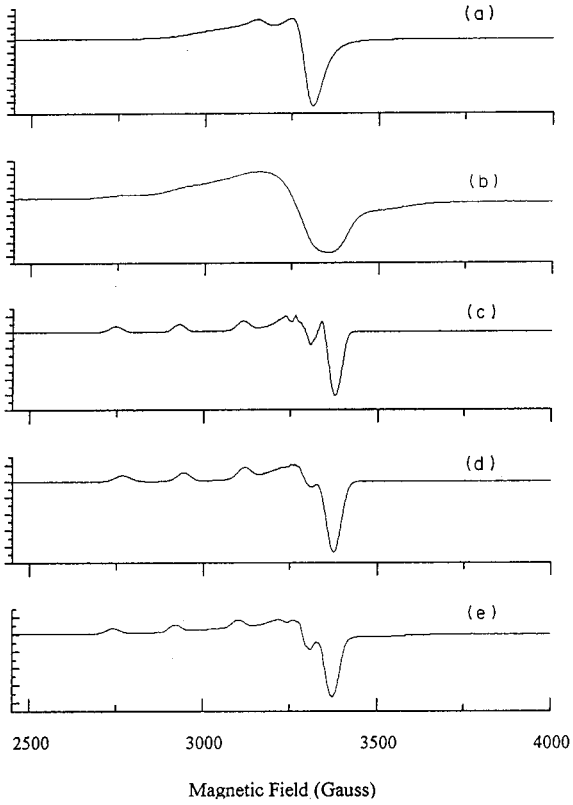

Figure 3. X-band EPR spectra of $Cu(salEen)_2(ClO_4)_2$ at 77 K: (a) polycrystals; (b) $CHCl_3$; (c) pyridine; (d) DMF; (e) MeOH.

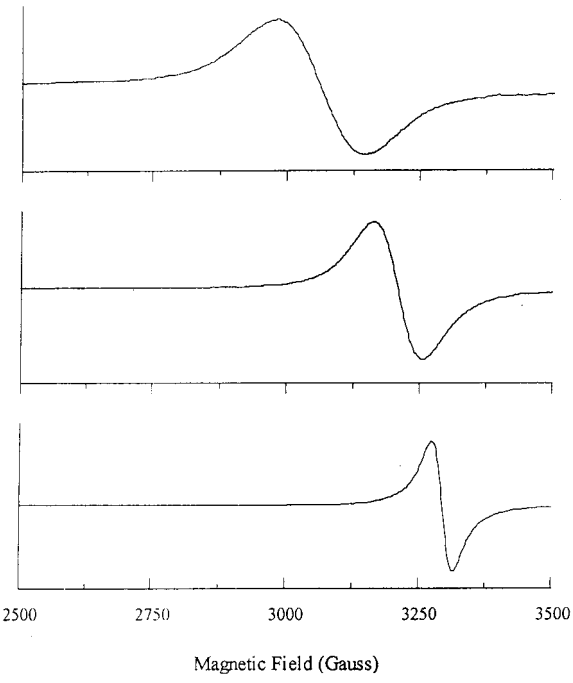

Figure 4. X-band EPR spectra of single crystals showing the anisotropy in line position and peak-to-peak line width at arbitrary orientations.

For a typical one-dimensional complex the spectral line shape is non-Lorentzian when the applied magnetic field is parallel to the chain axis and could be described by the Fourier transform of $\exp(-t^{3/2})$ time dependence.[27,28] However, when the chain axis makes a magic angle (54°44′) with respect to the applied field, the line shape is Lorentzian. The analysis indicated that the line shape of the EPR signal changes as a function of crystal orientation. The shape is more of Gaussian than Lorentzian.

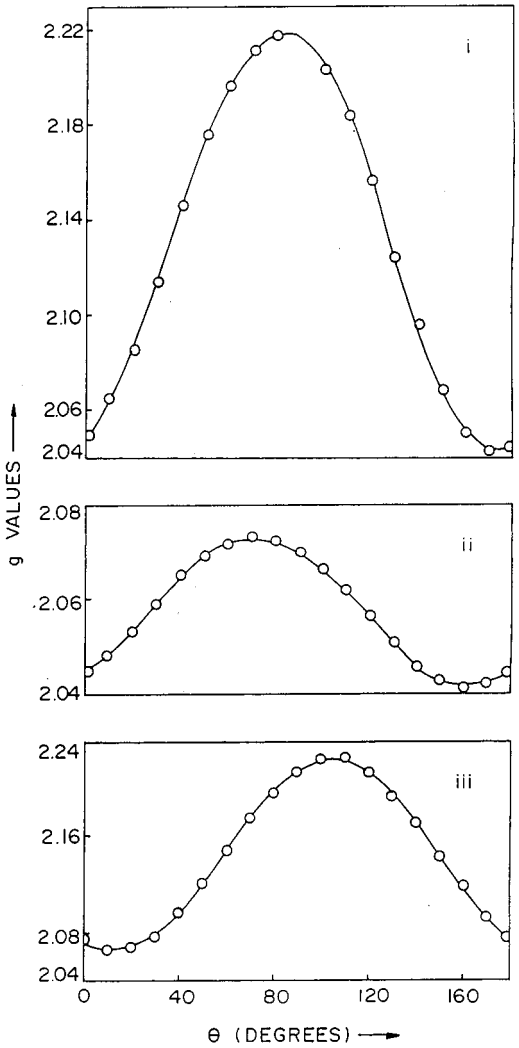

Figure 5. Angular variation of g values in three mutually perpendicular planes: (i) b^*c; (ii) ca^*; (iii) a^*b^*.

The observed EPR line width (ΔH) has contributions from both dipolar interactions, which broaden the signals, and exchange interactions, which narrow the signals. In three-dimensional magnetic systems, quite often the latter type of interactions dominate and the lines are exchange-narrowed. However, in one-dimensional systems the exchange effects are less effective and the line widths are between the exchange-narrowed and dipolar broadened limits. The spectra of one-dimensional systems are affected by the long time part of the spin correlation function, which is dominated by spin diffusion effects. In typical one-dimensional systems the angular variation of the line width follows a $|3\cos^2\theta - 1|^{4/3}$ dependence.[29−32] The line width of the resonance signal is indeed anisotropic and follows a $|3\cos^2\theta - 1|^{4/3}$ variation in all three planes. A

(27) Drumheller, J. E. *Magn. Reson. Rev.* **1982**, *7*, 123.
(28) Dietz, R. E.; Merritt, F. R.; Dingle, R.; Home, D.; Silbernagel, B. G.; Richards, P. M. *Phys. Rev. Lett.* **1971**, *26*, 1186.
(29) Ramakrishna, B. L.; Manoharan, P. T. *Mol. Phys.* **1984**, *52*, 65. Kuppusamy, P.; Manoharan, P. T. *Inorg. Chem.* **1985**, *24*, 3053. Venkatalakshmi, N.; Varghese, B.; Lalitha, S.; Williams, R. F. X.; Manoharan, P. T. *J. Am. Chem. Soc.* **1989**, *111*, 5748.
(30) Velayutham, M.; Varghese, B.; Subramanian, S. *Inorg. Chem.* **1998**, *37*, 5983.
(31) Towle, D. K.; Hoffman, S. K.; Hatfield, W. E.; Singh, P.; Chaudhuri, P. *Inorg. Chem.* **1988**, *27*, 394.
(32) Sanchis, M. J.; Gomez-Romero, P.; Folgado, J.-V.; Sapina, F.; Ibanez, R.; Beltran, A.; Garcia, J.; Beltran, D. *Inorg. Chem.* **1992**, *31*, 2915.

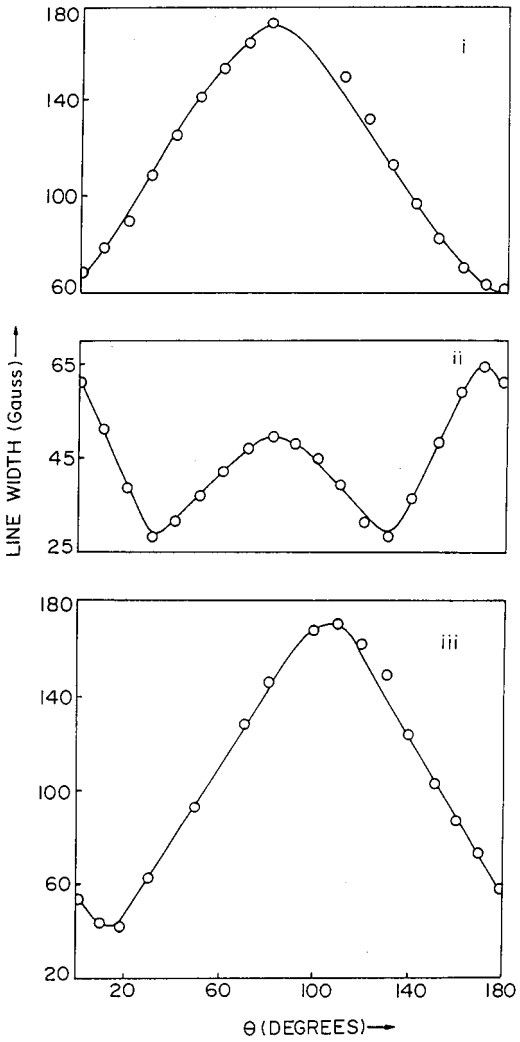

Figure 6. Angular variation of peak-to-peak line width in three mutually perpendicular planes: (i) b^*c; (ii) ca^*; (iii) a^*b^*.

maximum value of 175 G and a minimum of 28.2 G were observed at different crystal orientations. The intrabilayer Cu−Cu separation is more than the intralayer Cu−Cu separation, which is more than the interbilayer Cu−Cu separation. Since the dipole−dipole contribution to the EPR line width varies as r^{-6}, the magnitude of this interaction varies in the order interbilayer > intralayer > intrabilayer. For Cu−Cu separation of 6.49 Å, the contribution of dipole−dipole interaction to the line width is expected to be 360 G. A lower value of 175 G observed indicates that the exchange interactions also contribute to the line width. The variation of ΔH in all three orthogonal planes is shown in Figure 6.

EPR in Solutions. EPR spectra at 298 K and in various solvents show four equally spaced hyperfine features due to the interaction of electron spin ($S = {}^1/_2$) with the nuclear spin of copper ($I = {}^3/_2$). The resonances exhibit m_I-dependent line widths. The low-field hyperfine resonance is broader than the high-field resonance. Also, the intensity of the high-field resonance is more than the intensity of the low-field line. Isotropic g and A values evaluated by spectral simulation are listed in Table 3. The g_{iso} value is smaller for $CHCl_3$ than for the rest of the solvents and indicates a square planar coordination for Cu(II) in $CHCl_3$ and square pyramidal coordination in the rest of the σ-donor solvents. This observation agrees well the electronic spectral results (vide supra).

The spectra in strong σ-donor solvents (methanol, DMF, and pyridine) at 77 K resemble that of noninteracting monomeric species with well-resolved hyperfine features in the parallel region and partially resolved features in the perpendicular region. However, in CH_3CN or $CHCl_3$ the resonances are broad and the metal hyperfine features are barely seen or partially resolved (Figure 3). Additional features are observed in the region 3505−3535 G and at $g \approx 4.2$ (at higher spectrometer gain) typical of weakly interacting dimeric agglomerates in CH_3CN or $CHCl_3$ solutions.[33] These observations indicate that the complex retains dimeric association in weakly coordinating solvents. Strong donor solvents probably weaken this association because of solvolysis. The effect of solvent is more prominent on $g_{||}$ and $A_\perp$ values. Except for $CHCl_3$, the $g_\perp$ values for the rest of the solvents are invariant (Table 3).

Table 3. EPR Spin Hamiltonian Parameters for Polycrystals and Solutions of $Cu(salEen)_2(ClO_4)_2$ at 298 and 77 K[a]

state	temp, K	$g_{||}$ or g_z	$g_\perp$ or g_x, g_y	g_{iso}	$A_{||}$, G	$A_\perp$, G	A_{iso}, G
polycrystals	298	2.205	2.047				
			2.061				
	77	2.208	2.046				
			2.057				
$CHCl_3$	298			2.109			80.5
	77	2.225	2.070		179.7	NR	
pyridine	298			2.114			74.4
	77	2.226	2.054		176.4	11.9	
DMSO	298			2.117			74.5
	77	2.230	2.053		181.7	11.8	
DMF	298			2.114			80.1
	77	2.235	2.051		182.7	18.5	
methanol	298			2.117			76.5
	77	2.242	2.051		180.4	21.5	

[a] NR = not resolved. DMSO = dimethyl sulfoxide. DMF = *N*,*N*-dimethylformamide.

EPR spectra for the solid samples correspond to one-dimensional magnetic material bridged through perchlorato ions. However, in solutions the interconnectivities through counterions do not exist, but the bimolecular association due to interpenetration of the pendent arms and the $\pi-\pi$ stacking interactions of the bimolecular units are present, showing weak additional signals at $g \approx 4.2$.

^{1}H NMR Studies in Solutions. A majority of the copper(II) complexes either fail to give detectable NMR signals or give very broad, poorly resolved signals as a consequence of rapid nuclear spin relaxation induced by the paramagnetism.[10] Those complexes, which show narrow NMR signals coupled with isotropic shift, have very short electron relaxation times and are not good candidates for EPR studies. Among the copper complexes with coordination number 4, the square planar $Cu(acac)_2$ showed relatively broad NMR signals with isotropic shifts.[34] In contrast, bis(*N*-isopropylsalicylaldeiminato)Cu(II) with a psuedotetrahedral structure ($\theta = 60°$ in the solid state, where θ is the dihedral angle between the CuNO planes) exhibited a relatively well-resolved proton magnetic resonance (PMR) spectrum.[35] Bis(N-substituted β-ketoaminato)Cu(II) complexes also showed resolved PMR spectra.[36] In the case of dimeric Cu(II) complexes the electron spin exchange of the dimeric complexes provide a sufficiently efficient mechanism for electron spin relaxation, and thus the resolved PMR spectrum could be obtained.[11] Although $Cu(salEen)_2(ClO_4)_2$ is not a dimer

(33) Smith, T. D.; Pilbrow, J. R. *Coord. Chem. Rev.* **1974**, *13*, 173.
(34) Johnson, A.; Everett, G. W. *J. Am. Chem. Soc.* **1972**, *94*, 1419.
(35) Fritz, H. P.; Golla, B. M.; Keller, H. J.; Schwarzhans, K. E. *Z. Naturforsch.* **1966**, *21B*, 725.
(36) Holm, R. H.; O'Connor, M. J. *Prog. Inorg. Chem.* **1971**, *14*, 241.

Table 4. ^1H Chemical Shifts (δ) and Spin−Lattice Relaxation Times T_1 (in Parentheses in ms) of $Cu(salEen)_2(ClO_4)_2$ in Various Solvents

solvent	OH	phenyl protons	HC═N (azomethine)	ethylene	pendent ethyl
CD_3CN	12.4 (50)	6.96 (452), 7.41 (376)	8.58 (419)	3.45, 3.48, 3.50, 3.91, 3.93, 3.95	3.18, 3.20, 3.23, 3.25 (CH_2) 1.24, 1.28, 1.31 (CH_3)
DMSO-d_6	12.7 (104)	6.95 (360), 7.38 (354) 7.48 (273), 7.69 (361)	8.66 (362)	3.81, 3.83, 3.85	3.13, 3.16, 3.19 3.23 (190) 1.18, 1.22, 1.26 (373)
methanol-d_4	*a*	6.89, 6.93, 6.96 (149) 7.32, 7.36, 7.40, 7.44 (135)	8.62 (120)	3.51, 3.54, 3.57 (131) 3.97, 4.00, 4.02 (120)	3.35[a] 1.32, 1.36, 1.39 (141)
D_2O	*a*	6.90, 7.43	8.62	3.51, 3.99	3.05, 1.19

[a] Signals are broad or *J* coupling not resolved.

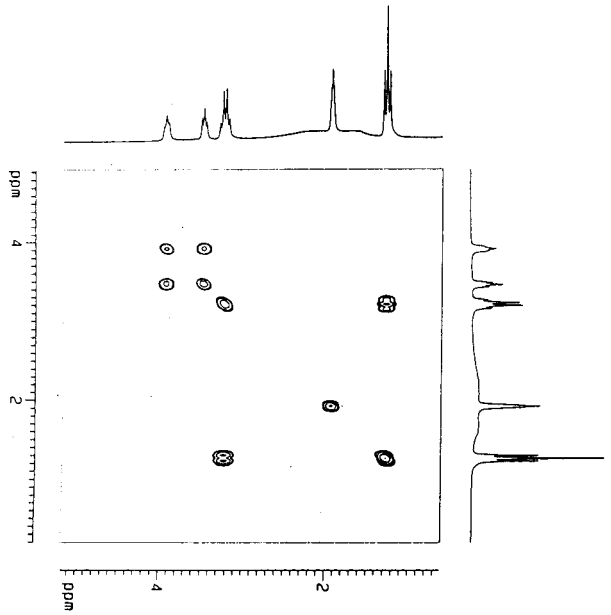

Figure 7. COSY-45 for $Cu(salEen)_2(ClO_4)_2$ in CD_3CN showing the proton connectivities.

in the true sense, it exhibits narrow PMR signals in CD_3CN at ambient temperatures. It is interesting to note that the present complex is amenable for both EPR and NMR studies. The line widths of the PMR signals increase with solvents in the order CD_3CN < DMSO-d_6 < methanol-d_4 < D_2O. The line width at half-maximum of the PMR signal could be correlated to the geometry around Cu(II). The narrow PMR signals in CD_3CN reveal that the geometry around Cu(II) is distorted square planar or pseudotetrahedral and that the bilayered molecular association of $Cu(salEen)_2(ClO_4)_2$ is stable even in the solution. On the other hand, the broader signals in DMSO-d_6, MeOH-d_4, and D_2O are due to solvent coordination forming square pyramidal geometry and weaker magnetic interaction between the bilayered units. Chemical shifts of PMR signals are solvent-sensitive, and the data are listed in Table 4.

Figure 7 shows the 2D correlation spectroscopy (COSY)-45 spectrum in CD_3CN revealing $^1H-^1H$ connectivities. The COSY spectrum shows ^3J coupling between the triplet at 1.31 δ and quartet at 3.35 δ for *N*,*N*-diethyl and between the triplet at 3.45 δ and 3.91 δ for ethylenic protons. Also, ^5J and ^3J connectivities were observed for aromatic protons of the "sal" group. The sharp PMR signals are consistent with the distorted square planar geometry for Cu(II) and agree well with the X-ray and EPR results. Although the complex is not dimeric, observation of narrow PMR signals is a notable feature.

Nuclear Spin−Lattice Relaxation Studies. Nuclear spin lattice relaxation studies of paramagnetic molecules provide the structural information. In the case of homodimers (e.g., Cu_2-Cu_2BESOD), where the exchange coupling constant $J \ll kT$, the decrease in nuclear spin lattice relaxation time is less than a factor of 2, while in strongly coupled systems such as ferridoxin, with $J \gg kT$, the reduction was by 3 orders of magnitude, as expected.[11] Surprisingly, in some weakly coupled dimeric Cu(II) systems the PMR signals were far too sharp and suggest new relaxation pathways sometimes created upon dimer formation. The molecular association and distorted square planar geometry in the present system has a marked effect on the proton spin lattice relaxation times. The T_1 values estimated using the inversion recovery method are listed in Table 5 along with the chemical shift parameters. Generally, organic ligands show T_1 in the range 1−10 s or longer, but these values for $Cu(salEen)_2$-$(ClO_4)_2$ in CD_3CN are small and are on the order of milliseconds. A gradual decrease of T_1 with electron−nucleus distance (r_{IS}) is observed. Phenolic OH has the shortest T_1 value (50 ms), while rest of the protons have T_1 values 9-fold larger than that for phenolic OH (355−450 ms). These results suggest that the pendent group *N*,*N*-diethyl is comparatively rigid because of molecular association, forming bilayers even in solutions. The solvent has a considerable effect on the T_1 value. The values are smaller in CD_3OD. Relatively broad signals were observed in D_2O.

Discussion

Although salEen can coordinate as a tridentate ligand through two N and one O atoms, the crystal structure of $Cu(salEen)_2$-$(ClO_4)_2$ reveals its coordination as bidentate through one N and one O atoms while the *N*,*N*-diethylethyleneamine group is left free. The pendent arm *N*,*N*-diethylethyleneamine participates in forming bimolecular aggregates. The geometry around copper is tetrahedrally distorted square planar. A similar distortion from square planar geometry was observed by us earlier for Cu(5-Cl-salen).[7] However, the magnitude of the distortion is more in the present complex than in Cu(5-Cl-salen).[7] Both the trans N atoms deviate from the mean plane of CuN_2O_2 to one side, while the trans O atoms deviate to the other side. The perpendicular deviation of atoms is larger (about ±0.36 Å) compared to that in Cu(5-Cl-salen) (about ± 0.11 Å).[7] The "sal" units are twisted with respect to each other (twist angle = 146.3°) and make angles of 167.3° and 36.2° with respect to the best plane of the donor atoms. In the case of Cu(5-Cl-salen) the "sal" units are twisted by 9.4° only and make angles of 11.5° and 8.2° with the best plane of the donor atoms. These observations indicate that the tetrahedral distortion is more in the present complex with a bidentate Schiff base ligand salEen than in the Cu(5-Cl-salen) having a tetradentate ligand. Similar distortions in square planar geometry were found in some salicylideaminato Cu(II) complexes.[37] Generally, the magnitude of tetrahedral distortion is measured in terms of the "fold" angle ϕ between

(37) Pilbrow, J. R.; Lowrey, M. R. *Rep. Prog. Phys.* **1980**, *43*, 435.

the CuNO plane and the best mean plane or θ, the dihedral angle between the planes CuNO. In $Cu(salEen)_2(ClO_4)_2$, these angles are found to be 14.9° and 30.1°, respectively. For a tetrahedral geometry the value of θ is about 90°, and for a planar geometry $\theta = 0°$. The value of 30.1° for θ in the titled complex reveals a geometry between square planar and tetrahedral. It is interesting to note such a tetrahedral distortion in type I blue copper proteins.[2,4]

UV−visible spectra in CH_3CN solutions showed a weak, broad band around 598 nm due to d−d transitions. This band for Cu(salen) type complexes appeared near 565 nm.[7] A red shift of the d−d band for $Cu(salEen)_2(ClO_4)_2$ is consistent with the tetrahedrally distorted square planar geometry revealed by the X-ray crystal structure. Also, the rhombic g values for polycrystalline samples are in agreement with this geometry. The lower copper hyperfine coupling (A_{iso}, $A_{||}$, and $A_{\perp}$) parameters for $Cu(salEen)_2(ClO_4)_2$ (Table 3) compared to Cu(salen) could be explained by the following two reasons. (1) The tetrahedral distortion of the square planar geometry admixes the "formal" $3d_{x^2-y^2}$ orbital ground state with the $3d_{z^2}$ orbital and thereby causes reduction in the copper hyperfine coupling constant.[38,39] (2) Delocalization of spin density onto the ligands is more in $Cu(salEen)_2(ClO_4)_2$ than in Cu(salen) complexes. This agrees well with the shorter Cu−O bonds (Cu1−O1 = 1.884(5) Å and Cu1−O2 1.876 Å) in $Cu(salEen)_2(ClO_4)_2$, corresponding to a closer approach of the ligand moiety for a much stronger chelate coordination with Cu(II). In other words, both tetrahedral distortion and stronger chelate coordination are responsible for reduction in copper hyperfine coupling constants.

The peak-to-peak line width variation in the three orthogonal planes is indicative of one-dimensitional magnetic behavior. It is obvious from the crystal packing diagram (Figure 2) that counterion ClO_4^- makes strong contacts with the adjacent cation moiety and that these interactions are responsible for the one-dimensional magnetic behavior of $Cu(salEen)_2(ClO_4)_2$. In addition to this, the $\pi-\pi$ stacking interactions of phenyl rings and bimolecular aggregation also contribute to the magnetism. The weak additional signals in the region 3505−3535 G and half-field signal ($g \approx 4.2$) in $CHCl_3$ and CH_3CN solutions give evidence for the bimolecular association even in solutions. The red shift of the d−d band and larger $g_{||}$ values in pyridine, DMSO, DMF, and methanol suggest solvent coordination and formation of square pyramidal complexes.[1] The PMR spectra are in good agreement with UV−visible and EPR results. Narrow PMR signals for CD_3CN correspond to tetrahedrally distorted square planar Cu(II) geometry, while broader signals in DMSO-d_6, methanol-d_4, and D_2O are due to square pyramidal geometry. Observation of both sharp NMR signals and EPR signals at 77 K for $Cu(salEen)_2(ClO_4)_2$ could therefore be explained as being due to (i) a significant amount of electron delocalization onto the ligand, (ii) a distorted square planar geometry for Cu(II), and (iii) weak magnetic interactions in the bimolecular unit.

The tetrahedrally distorted square planar geometry for blue copper proteins is responsible for its unique spectral characteristics and reactivity. The chloro-substituted Cu(salen) complex showed higher catalytic activity than Cu(salen) in the selective, low-temperature oxidation of *p*-xylene and phenol.[40] Also the rates of decomposition of hydrogen peroxide and *tert*-butyl hydroperoxide are more for Cu(5-Cl-salen). The higher reactivity of Cu(5-Cl-salen) compared to Cu(salen) is due to its tetrahedrally distorted square planar geometry and admixed ($d_{x^2-y^2}$/d_{z^2}) ground state. The analogous complexes of the present type with dimethyl substitution exhibited catalytic activity in the epoxidation of alkenes by molecular oxygen and 2-methylpropanol.[12] The present complex with more tetrahedral distortion than that of Cu(5-Cl-salen) is therefore expected to be more active, and experiments in this direction are in progress. Molecular association with two copper ions coming together is an added advantage of $Cu(salEen)_2(ClO_4)_2$. Both copper sites could simultaneously participate in the catalysis to oxidize suitable substrate molecules. This probably opens up a new dimensionality for this molecule in the field of catalysis.

Conclusions

$Cu(salEen)_2(ClO_4)_2$ complexes exhibit a novel one-dimensional structure. The pendent arms *N*,*N*-diethylethylenediamine from two copper units in the adjacent layers interpenetrate and form a bilayered structure with large cavities. Two such bilayers come closer with a Cu−Cu distance of 6.49 Å, and this molecular association is persistent even in noncoordinating solvents, as revealed by EPR spectra at 77 K. The geometry of copper is tetrahedrally distorted square planar with N_2O_2 coordination. EPR spectra for single crystals are consistent with the one-dimensional magnetic behavior. Nuclear spin lattice relaxation times are remarkably short and suggest rigidity for the pendent arm because of interpenetration. The observation of both EPR and NMR spectra at ambient temperatures is an interesting feature of this complex.

Acknowledgment. The authors thank Dr. Babu Varghese, IIT, Chennai for the help in crystal morphology determinations.

Supporting Information Available: X-ray crystallographic files in CIF format, eight tables listing data for $Cu(salEen)_2(ClO_4)_2$, and a figure showing the solvent effect on the UV−visible spectrum. This material is available free of charge via the Internet at http://pubs.acs.org.

IC990874Q

(38) Srinivas, D.; Swamy, M. V. B. L. N.; Subramanian, S. *Mol. Phys.* **1986**, *57*, 55.
(39) Jacob, C. R.; Varkey, S. P.; Ratnasamy, P. *Appl. Catal. A* **1999**, *182*, 91.
(40) Deshpande, S.; Srinivas, D.; Ratnasamy, P. *J. Catal.* **1999**, *188*, 261.